Journal of Physiology (1991), **434**, *pp.* 23–40
With 8 figures
Printed in Great Britain

THE CONTRIBUTION OF THE 'PACEMAKER' CURRENT (i_f) TO GENERATION OF SPONTANEOUS ACTIVITY IN RABBIT SINO-ATRIAL NODE MYOCYTES

BY DARIO DIFRANCESCO

From the Università di Milano, Dipartimento di Fisiologia e Biochimica Generali, Elettrofisiologia, via Celoria 26, 20133 Milano, Italy

WITH AN APPENDIX BY D. NOBLE*, J. C. DENYER* AND D. DIFRANCESCO

(*Received 10 April 1990*)

SUMMARY

1. The contribution to the diastolic depolarization of the hyperpolarization-activated current, i_f, relative to other components was investigated in isolated rabbit sino-atrial (SA) node myocytes.

2, During the diastolic phase the membrane potential depolarized by $0{\cdot}1096 \pm 0{\cdot}014$ V/s, which requires only about 3 pA of inward current in a cell with an average capacity of 30 pF. The problem of which ionic component is responsible for initiating the diastolic depolarization was investigated by analysing the composition and the properties of the net inward current in the diastolic range of voltages.

3. The measured instantaneous 'background' current activated during voltage clamp steps from a holding potential of -35 mV was outward positive to approximately -61 mV, and had a region of negative slope conductance from -45 to -35 mV.

4. The instantaneous component lost its rectifying behaviour in the presence of Ni^{2+} (100 μM) and nitrendipine (10 μM). These blockers of Ca^{2+}-dependent currents modified the instantaneous I–V relation at voltages positive to -45 to -50 mV, thus implying that Ca^{2+} currents become important at less negative potentials than -50 mV, towards the very end of diastolic depolarization.

5. Possible errors introduced by voltage clamp analysis with the whole-cell method on the instantaneous current and on i_f measurement were evaluated. Leakage through the seal resistance caused the instantaneous I–V relation to be displaced in the inward direction at negative voltages. Correction for the seal leakage moved the reversal potential for the instantaneous current toward the negative direction from -61 to approximately -66 mV. Thus, no depolarization can be driven by the background current beyond -66 mV.

6. During voltage clamp analysis, lack of series-resistance compensation led to lack of intracellular voltage control, as was apparent using a second pipette on the same cell. This slowed activation of i_f and led to a 1·5- to 2-fold reduction of i_f size

* University Laboratory of Physiology, Parks Road, Oxford.

MS 8421

in the range -55 to -115 mV. Thus, uncorrected measurements of the instantaneous component and of i_f may concur to underestimate the role of i_f in pacemaking.

7. These results lead to the conclusion that in the SA node cells analysed, pacemaker activity is generated with the essential contribution of the hyperpolarization-activated current, i_f. Numerical computation of SA node cell activity using an extension of the DiFrancesco–Noble model shows that the i_f-activation hypothesis can account for the presence of spontaneous action potentials and their sensitivity to i_f changes.

INTRODUCTION

Spontaneous activity in SA node cells is controlled by the slow diastolic ('pacemaker') depolarization. During this phase the membrane voltage is driven from the maximum level of hyperpolarization (maximum diastolic potential, MDP) reached at the termination of an action potential up to threshold for the initiation of a new action potential. What is the mechanism controlling the diastolic depolarization? Obviously, this process requires that the net ionic current turns from outward to inward at the MDP. There are two main hypotheses to explain the onset of a net inward current at the MDP: (a) the 'i_K-decay' hypothesis, based on the presence of an inward background current which is unmasked by the decay of the potassium current, i_K, that follows repolarization of the action potential, a process itself driven by i_K activation (for references see Irisawa, 1978, 1987; Brown, 1982; Brown, Kimura, Noble, Noble & Taupignon, 1984; Noble, 1984; and (b) the 'i_f-activation' hypothesis, based on the assumption that the process initiating the slow diastolic depolarization is the activation of the hyperpolarization-activated current, i_f (DiFrancesco, 1985; DiFrancesco & Noble, 1989). A third possibility, activation of Ca^{2+} currents, is less likely because in SA node cells both L- and T-type currents activate at voltages too positive to initiate the slow diastolic phase (i.e. positive to -50 mV; Hagiwara, Irisawa & Kameyama, 1988)

The 'i_K-decay' and 'i_f-activation' hypotheses do not differ in the assumption that the current i_K decays during the first fraction of pacemaker depolarization. Onset of the current i_K is responsible (together with any outward 'background' component) for the repolarizing phase of the SA node action potential (see for example DiFrancesco & Noble, 1989), and its termination is accompanied by switch-off of the current i_K which proceeds along with the development of the diastolic depolarization. The two hypotheses differ rather in the assumption that the inward component which balances i_K at the MDP and which eventually overtakes i_K and drives the diastolic depolarization is a 'background' component or is the hyperpolarization-activated current i_f.

In this paper the composition of the net inward current in the diastolic range is analysed in isolated SA node myocytes with the aim of determining the contribution of different components to the generation of the pacemaker depolarization. The results indicate that there is no net inward current at voltages in the diastolic depolarization range (about -60 to -35 mV) and the only inward contribution able to initiate this phase in spontaneously beating SA node myocytes appears to be due to i_f activation.

METHODS

Isolation of single cardiac myocytes from rabbit sino-atrial node preparations was performed as described previously (DiFrancesco, Ferroni, Mazzanti & Tromba, 1986; DiFrancesco & Tromba, 1988*a*, *b*). In brief, hearts were extracted from 0·9–1·0 kg rabbits killed under tribromoethanol anaesthesia by a blow on the head and exsanguination, and strips were cut from the SA node region and left to recover spontaneous activity in normal Tyrode solution containing (in mM): NaCl, 140; KCl, 5·4; $CaCl_2$, 1·8; $MgCl_2$, 1; D-glucose, 20; HEPES-NaOH, 5 (pH = 7·4). After exposure to a zero-Ca^{2+}, low-Mg^{2+} solution containing (mM): NaCl, 140; KCl, 5·4; $MgCl_2$, 0·5; KH_2PO_4, 1·2; D-glucose, 5·5; taurine, 50; HEPES-NaOH, 5 (pH = 6·9), tissue digestion was performed by shaking the strips for 20–30 min in the same solution containing 0·2 mM-$CaCl_2$, 1 mg/ml albumin and the following enzymes: type I collagenase, 570 U/ml; protease, 0·5 U/ml; elastase, 1·9 U/ml. Collagenase was from Worthington Biochem, USA and protease and elastase were from Sigma, USA. Cells were separated by shaking the pieces for 15 min in a solution containing (mM): KCl, 20; KH_2PO_4, 10; KOH, 70; β-hydroxybutiric acid, Na salt, 10; glutamic acid, 70; taurine, 10; HEPES-KaOH, 10 (pH = 7·4); and albumin, 1 mg/ml, and were stored for the day in a solution containing (mM): NaCl, 100; KCl, 35; $CaCl_2$, 1·3; $MgCl_2$, 0·7; HEPES-NaOH, 5 (pH = 7·4); and albumin, 1 mg/ml, after calcium adaptation. Experiments were performed superfusing cells settled in Petri dishes with normal Tyrode solution at 35–36 °C. Whole-cell current and voltage clamping was performed with pipettes filled with an intracellular-like solution containing (mM): NaCl, 10; potassium aspartate, 130; Mg-ATP, 2; $CaCl_2$, 2; EGTA, 5; GTP, 0·1; HEPES-KOH, 10 (pH = 7·2). In normal Tyrode pipettes had a mean resistance of $3·02 \pm 0·23$ MΩ ($n = 12$). Solution changes were rapid (less than 1 s) and were obtained with a superfusion pipette described previously (DiFrancesco & Tromba, 1988*a*). Voltage and current traces were recorded on PCM-video recording system and played back on a 12-bit digital oscilloscope (Nicolet, USA) interfaced to an Olivetti M380 desk computer for subsequent analysis. The 'instantaneous' component in Figs 2, 3, 4 and 5 was measured with hyperpolarizing pulses from the holding potential of −35 mV. This protocol satisfies three conditions: (1) the holding level of −35 mV minimizes activation of time-dependent currents (i_f, i_K, Ca^{2+} currents) and therefore their contribution to the instantaneous current measurement; (2) both the instantaneous and i_f components can be simultaneously measured, and (3) dissection of the time-dependent i_f activation from the much faster capacitative transient can be easily accomplished. All software for data collection and analysis was developed in our laboratory. The data reported in this paper are based on seventeen experiments and a total 112 cells was analysed.

RESULTS

Size of inward current necessary for pacemaker activity

The relation $I_t = I_i + I_C = 0$, where I_t is total current and I_i, I_C are the net ionic and capacitative currents, holds during spontaneous activity. Thus in single-cell preparations, the absolute size of net ionic current is related to the rate of change of voltage for a uniform cell by the equation

$$I_i = -C\frac{dV}{dt}. \quad (1)$$

The ionic current flowing during activity can thus be easily assessed by measurement of the cell capacity, C, and of the voltage time course $V(t)$. In Fig. 1 the spontaneous activity (A) and the ionic currents recorded in the same SA node myocyte on clamping to a voltage range (−65 to −45 mV, C) comprising the diastolic depolarization are shown.

Voltage clamp steps were applied from the holding potential of −35 mV and the currents developing during the first 200 ms, a time comparable with that of the

diastolic depolarization, give an indication of the components involved in the cell's spontaneous activity. For a more detailed analysis, however, it is necessary to compare quantitatively the currents measured during voltage clamp with the net ionic current actually required to generate the autonomous activity. The cell shown

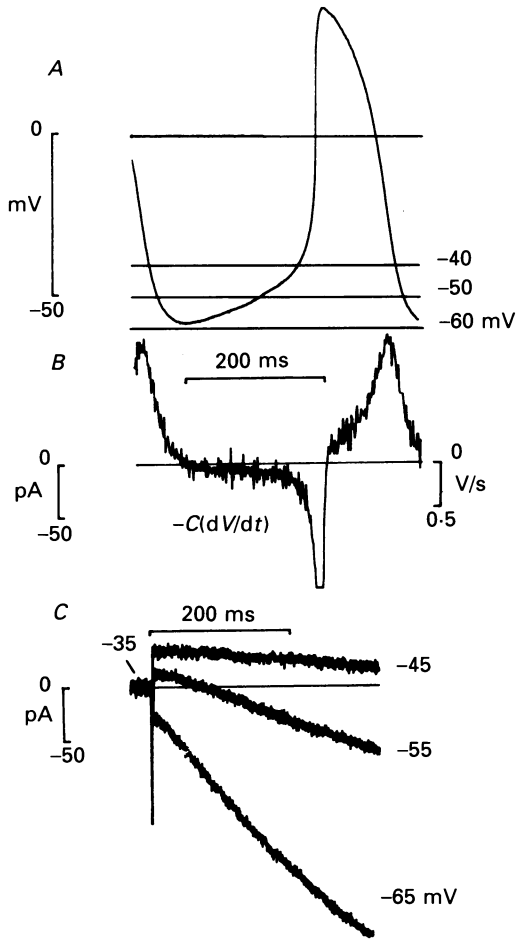

Fig. 1. Comparison between ionic current flow during activity and currents recorded during voltage clamp. *A*, spontaneous activity recorded in current clamp mode in a single myocyte. The diastolic depolarization develops within the range −60 to −40 mV. *B*, voltage derivative obtained digitally by differentiating the voltage trace. This record also represents the time course of net ionic current flowing during activity, as calculated using the relation $I_i = C(dV/dt)$ with the cell capacity of 72 pF. *C*, current traces recorded in the same cell during voltage clamp steps to the levels indicated from a holding potential of −35 mV. Notice that the instantaneous 'background' component reverses between −55 and −60 mV, and that it cannot contribute to depolarize the membrane at voltages positive to its reversal potential.

in Fig. 1 had a capacity of 72 pF, from which using the above relation (1), a simple numerical differentiation of the voltage record yielded the trace shown in panel *B* of Fig. 1. This comparison is particularly instructive when considering the pacemaker

depolarization, because it shows that the size of the current flowing during this phase is indeed small. For the cell in Fig. 1 this is in the range of −7 pA, which corresponds to the mean measured diastolic slope of approximately 0·1 V/s with the cell capacity of 72 pF. The mean slope of diastolic depolarization from six cells was 0·1096±0·0142 V/s, which in a cell with a mean capacity of about 30 pF (DiFrancesco, 1986) requires approximately as little as −3 pA. The records in Fig. 1 also show that while i_f develops to values that exceed those necessary to underlie the diastolic depolarization, no instantaneous inward current exists at −45 and −55 mV, and no inward contribution can therefore be supplied by this component positive to −55 mV. It is therefore essential for the estimation of the contribution of various ionic components to the slow diastolic depolarization that accurate current measurements (within the range of few picoamperes only) are made in the relevant voltage range. It is interesting to note that using a similar experimental protocol, van Ginneken (1987) showed that the computed time course of i_f developing during pacemaker depolarization almost overlapped the $-C(dV/dt)$ trace in a single cell, in agreement with the view that the amount of i_f involved is sufficiently large to drive the pacemaker depolarization by itself. It is also clear that, while the data in Fig. 1*C* give an indication of the size of i_f activated during voltage clamp steps to the diastolic range, a proper calculation of the amount of current involved in the pacemaker depolarization can only be obtained by numerical computation (see Figs 7 and 8).

Determinants of the net inward current flowing during the diastolic depolarization

According to the relation $I_i = -C(dV/dt)$, at the maximum diastolic potential (MDP) the total ionic current is zero and turns from net outward to net inward. The net inward current that develops after the MDP then drives the slow diastolic depolarization. These elementary observations indicate the conditions that any current generating the slow diastolic depolarization (which can be referred to as 'pacemaker current') must satisfy: (a) it must be an inward current and (b) it must be activated upon hyperpolarization to the MDP range. To identify the component(s) sharing these properties and thus contributing to the diastolic depolarization, it is therefore important to analyse the nature of the current elicited by hyperpolarizing steps to the diastolic voltage range.

In the experiment shown on Fig. 2*A*, steps were applied from a holding potential of −35 mV and the time-dependent and time-independent currents were analysed after subtraction of the capacitative component. In this cell the instantaneous current *I–V* relation showed, as in the cell of Fig. 1, a range of negative conductance (from −35 to −45 mV) and reversed at about −64 mV.

The 'instantaneous' component, or 'background' component, is here referred to as the overall time-independent current, or the current that is left after all time-dependent contributions have been subtracted. This current is given by the net contribution of several different time-independent components. Clearly, only the algebraic sum of all contributions is important in determining the time derivative of voltage during activity. Plotting the instantaneous component (i_b) and the time-dependent (i_f) component activated after either 100 or 200 ms (*A*, right) shows that the fraction of net inward current contributed by i_f is predominant over that

contributed by the background component over the whole of the pacemaker voltage range. This simple result illustrates the important point that, at least down to −64 mV, there is no inward background current and all of the time-dependent inward current is attributable to i_f. Also, the size of i_f activated at times comparable

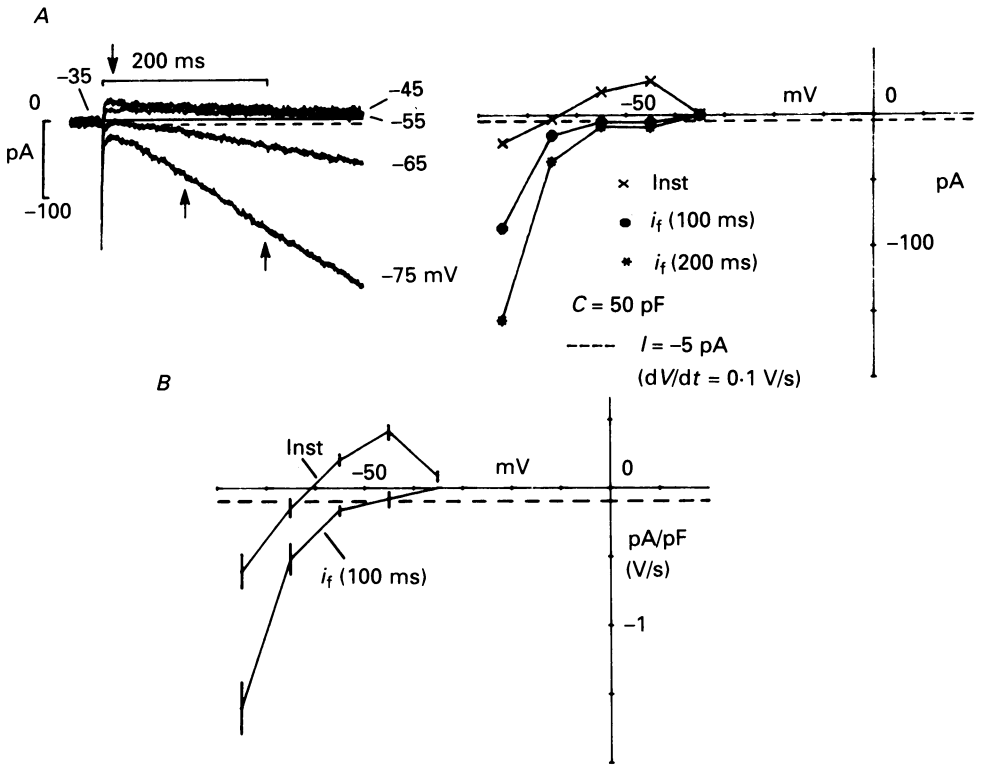

Fig. 2. Comparison between contributions of the instantaneous current and i_f in the diastolic voltage range. *A*, current traces (left) and corresponding *I–V* relations (right) obtained upon hyperpolarization to the levels indicated. Curves shown are the mean of three records. Capacitative components were subtracted by analogic correction. Values measured at 10 ms (Inst, ×), 100 ms (●) and 200 ms (*) after pulse onset are plotted. Cell capacity was 50 pF, and in both plots the dashed line represents the current level of −5 pA, required to drive a hypothetical pacemaker depolarization of 0·1 V/s. *B*, mean instantaneous (Inst) and i_f (100 ms) *I–V* relations from six cells normalized to cell capacity. Mean ± S.E.M. values are plotted on a pA/pF scale, which is dimensionally equivalent to a V/s scale. The level of 0·1 V/s is indicated by a dashed line.

with the duration of diastolic depolarization is certainly sufficient to drive this phase. This is clear if one compares the amount of i_f activated with the current level required to drive a diastolic depolarization of 0·1 V/s, indicated by a dashed line in both panels of Fig. 2*A*. Thus, in this cell any kind of pacemaking with MDPs not exceeding −64 mV would be driven exclusively by i_f activation. Similar results were obtained in five other cells.

In Fig. 2*B* the instantaneous *I–V* relation and the *I–V* relation for i_f at 100 ms averaged from six cells after normalization to cell capacity are shown. The reversal

potential of the mean instantaneous component was −61 mV, and the voltages at which the instantaneous component and i_f (after 100 ms) reached the level of 0·1 pA/pF (dashed line, corresponding to a voltage derivative of 0·1 V/s) were −63·5 and −47·5 mV, respectively.

These results indicate that the mean instantaneous current is outward at voltages more positive than −61 mV. However, more negative MDPs can be recorded (DiFrancesco *et al.* 1986; DiFrancesco & Tromba, 1988*a*), and the possibility that a contribution from an instantaneous component is present cannot be excluded, although clearly by far the largest contribution comes from i_f. As shown later, however, correcting for the leakage component further shifts the inward current reversal potential to more negative voltages (Fig. 5 below).

Lack of contribution of the current i_K to the instantaneous component

The holding potential of −35 mV used in the experiment of Fig. 2 is at the bottom of the activation range of the K current i_K (DiFrancesco, Noma & Trautwein, 1970), and a possible contribution of i_K to the instantaneous current measured from this potential could therefore be present.

To evaluate the extent of this possible interference from i_K, the current instantaneous jump was measured under conditions where the contribution of time-dependent components can be excluded. This is shown in Fig. 3. Here, the *I–V* relation for i_b obtained with standard protocol (panel *A*, as in Fig. 2) was compared with the instantaneous curve measured with trains of steps of 10 ms duration applied every 30 ms (panel *B*). At this frequency, current changes due to i_K, which has a time constant of about 200 ms at −40 mV (DiFrancesco & Noble, 1989), are obviously minimized. The increase in frequency of pulse delivering did not appear to affect the instantaneous *I–V* relation, which was nearly identical to that measured in standard conditions (panel *C*). According to the evidence in Fig. 3, the voltage dependence of i_b measured from a holding potential of −40 mV does not appear to be dependent on i_K. The level of −35 mV was preferred to a more negative level in order not to activate i_f (see DiFrancesco & Noble, 1989, Fig. 2). In two cells where the holding potential was −35 mV, i_b still displayed the same kind of voltage dependence as in Fig. 2 (data not shown), which further supports the independence of the instantaneous *I–V* relation from the delayed K^+ current.

Instantaneous contribution of Ca^{2+} currents

In the previous section it has been shown that the instantaneous background current is outward in the range −61 to −35 mV, which rules against the existence of a Na^+-dependent inward component large enough to drive the pacemaker depolarization, as required from the i_K-decay hypothesis. In this section the possible contribution to the instantaneous jump of Ca^{2+}-dependent currents is analysed. L- and T-type Ca^{2+} currents have been described in SA node cells (Hagiwara *et al.* 1988). Both components are activated on depolarization from threshold voltages of about −30 and −50 mV for the L-type and T-type, respectively (Hagiwara *et al.* 1988), and although it is known that the final fraction of pacemaker depolarization is affected by changes in the Ca^{2+}-dependent currents (Brown *et al.* 1984), a time-

dependent contribution at voltages near the MDP can be discarded, both because of the voltage range involved and the fact that Ca^{2+}-dependent currents are activated on depolarization, rather than on hyperpolarization. Given the small size of currents involved, however, it is important to investigate the possible existence of a time-

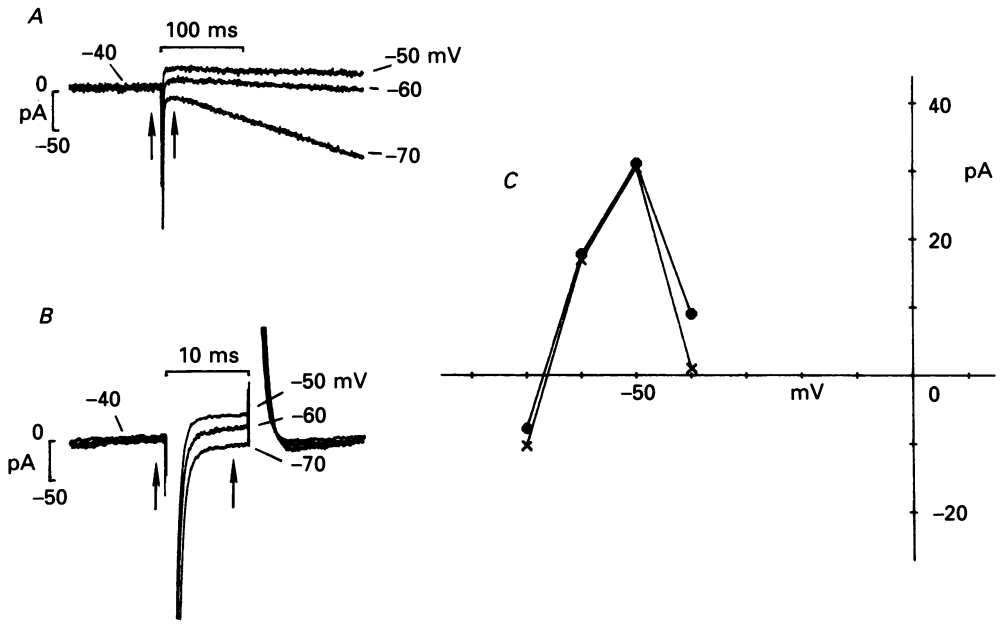

Fig. 3. Instantaneous current measured during pulse trains. *A*, current elicited on hyperpolarization to the voltages indicated using the same protocol as in Fig. 2 from the holding potential of −40 mV. *B*, current during trains of voltage steps applied at a frequency of 33 Hz (30 ms intervals) to the levels indicated. The average of more than five traces is shown for each record. The current was measured at the time indicated by the arrow, after the cell capacity was fully discharged. *C*, *I–V* relations measured for the protocol in *A* (●) and in *B* (×) at the times indicated by arrows.

independent contribution which could be present if, as for the cardiac Na^+ current (Attwell, Cohen, Eisner, Ohba & Ojeda, 1979), Ca^{2+} currents also displayed a steady-state 'window' component. In this case, hyperpolarization could elicit a Ca^{2+}-dependent inward current. Figure 4 shows the action of nitrendipine (10 μM) and $NiCl_2$ (100 μM) on the instantaneous current.

At these concentrations nitrendipine (a compound similar to nifedipine) and Ni^{2+} should abolish the L- and T-type current, respectively, in SA node cells (Bean, 1985; Hagiwara *et al.* 1988). As Fig. 4 illustrates, in the presence of the blocking agents the instantaneous *I–V* relation loses its negative slope region, which is thus to be attributed to the Ca^{2+}-dependent components. No obvious change occurs, on the other hand, at voltages below approximately −45 mV, indicating that there is no contribution of Ca^{2+} currents in the MDP range. Similar results were obtained in nine more cells. The threshold for the nitrendipine- and nickel-dependent component varied between 45 and −50 mV. These data confirm previous results suggesting that

Ca^{2+} currents do not affect the initial part of the pacemaker depolarization (Brown *et al.* 1984; DiFrancesco & Noble, 1989), and indicate that they are not responsible for initiating this phase.

Subtraction of leakage conductance

The measured reversal potential for the instantaneous current, $E_{inst} = -61$ mV, is more positive than E_K (about -80 mV), which suggests that we are not dealing with

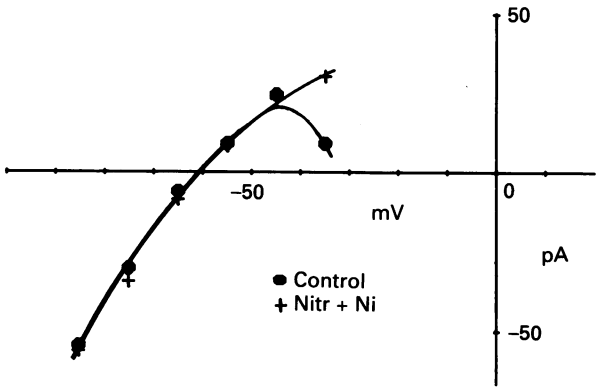

Fig. 4. Instantaneous *I–V* relation measured in a cell in a control solution (●) and after addition of 10 μM-nitrendipine (Nitr) and 100 μM-$NiCl_2$ (+). Evidence for an instantaneous 'window' component implies that in the range around -35 mV a small fraction of Ca^{2+} current is activated at steady state. Curves drawn by eye.

a pure K^+ component, but with a mixed ionic current. However, the measured E_{inst} is in fact more positive than the real one if one takes into account the leakage conductance due to pipette sealing. Dissection of the contribution due to leakage also decreases the size of the instantaneous component in the MDP range, as illustrated in Fig. 5.

During voltage clamp, the presence of leakage adds an ohmic component to any recorded current trace. If leakage does not change when passing from the cell-attached to the whole-cell configuration, this component should correspond to the leakage through the seal resistance seen in the cell-attached configuration prior to rupturing the membrane. The seal resistance varied in the range 2–12 GΩ, and was $5{\cdot}096 \pm 0{\cdot}516$ GΩ (mean ± S.E.M) from measurements in the twenty-five cells.

In Fig. 5*A* the instantaneous *I–V* relation for a single cell is shown before (×) and after (■) subtraction of leakage generated by a seal resistance of 5 GΩ. E_{inst} was shifted from -61 to -66 mV (top). The mean instantaneous *I–V* relation of Fig. 2*B*, re-plotted in Fig. 5*B*, reversed at -66 mV after the same correction, with a -5 mV shift with respect to the uncorrected curve.

As a whole, these results indicate that a contribution of 'background' components to the generation of pacemaker depolarization at voltages in the normal MDP range is unlikely. The reversal potential of the instantaneous current also suggests that a substantial fraction of the time-independent component is carried by K^+ ions.

Limitations in the measurement of i_f due to series resistance

In the previous sections evidence has been collected showing that (1) the instantaneous *I–V* relation measured from −35 mV is outward positive to −66 mV with a region of negative slope conductance (see also Denyer, 1989), and (2) steady

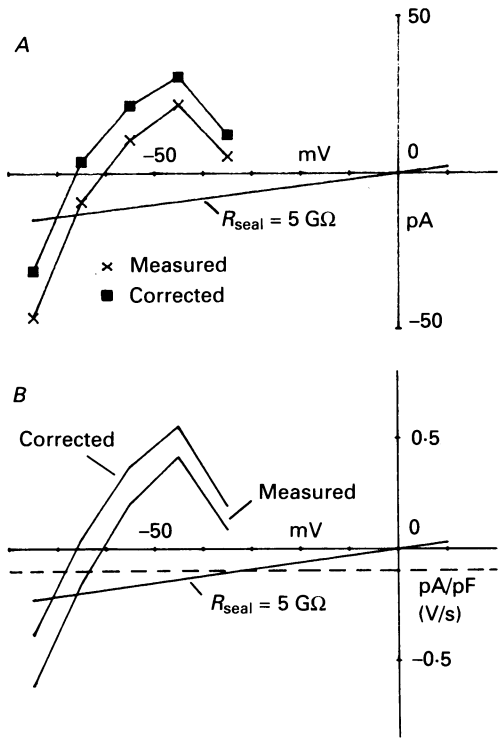

Fig. 5. Correction of instantaneous *I–V* relation for the leakage through seal resistance. *A*, instantaneous I–V plot measured at 10 ms after onset of hyperpolarizing steps from −35 mV (×). Subtraction of a linear component attributable to a leakage through a seal resistance of 5 GΩ (straight line) leads to a 'corrected' *I–V* relation (■). *B*, mean *I–V* relations for the instantaneous component measured in six cells (same as in Fig. 2) and after correction for a seal resistance of 5 GΩ, as indicated. Only curves through experimental points have been drawn for clarity. The reversal potentials were −61 and −66 mV for the measured and corrected *I–V* relations, respectively. The level of 0·1 V/s is marked by a dashed line.

Ca^{2+}-dependent currents are activated at voltages more positive than about −45 mV. Thus, in cells where both conditions are satisfied, neither the background current nor the Ca^{2+} currents are available for initiating the pacemaker depolarization, which is then solely controlled by i_f activation.

During activity, the amount of i_f available at the MDP will obviously depend on the exact position of the current activation curve and on its rate of activation. These properties are variable from cell to cell due to natural variability and to the run-down phenomenon (DiFrancesco *et al.* 1986; DiFrancesco & Noble, 1989). Quite apart from this variability, the amount of i_f available at negative potentials can be

seriously underestimated by the presence of an uncompensated series resistance during whole-cell voltage clamping. An example of this distortion is given in Fig. 6.

In this experiment two pipettes were used in the whole-cell configuration on the same myocyte, and voltage clamp steps were delivered through one pipette while the second pipette was used to record voltages, as illustrated in Fig. 6*C*. The arrangement shown allows measurement of the series resistance of the voltage-delivering pipette and assessment of the degree of distortion introduced by it. When an uncompensated series resistance is present, the voltage sensed by the membrane can vary dramatically during a step if large changes in the membrane conductance are present, as in the case of i_f activation on hyperpolarization. If the membrane is represented as a parallel of a time-independent (background, R_b) and a time-dependent (R_f) element in series with the series resistance R_s (Fig. 6*C*), it can be easily shown that the membrane potential V_m is expressed as

$$V_m = V_c/(1+R_s/R_b+R_s/R_f), \tag{2}$$

where V_c is the applied command voltage (see Appendix A). In this relation the membrane capacity has been ignored on the assumption that the time-dependent ionic current changes are much slower than the charging of membrane capacity. According to relation (2), during activation of i_f the fraction of voltage sensed by the membrane will decrease with time as a result of channel opening and of the increase of the membrane conductance. This effect will obviously be larger the larger the ratio R_s/R_f. In Fig. 6, applying a series of step hyperpolarizations of amplitudes ranging from 20 to 80 mV results in marked deflections of the membrane voltage measured by the voltage-sensing pipette. For example, during the −80 mV step the measured membrane voltage decreased from about −71 to −64 mV in 1 s. As predicted by relation (2), the time course of membrane voltage mirrored that of i_f activation. Introducing a correction for the series resistance resulted in a larger i_f and a reduction of V_m decay (Fig. 6*A* and *B*, middle panels). A complete series-resistance compensation was not possible, however, due to oscillation of the amplifier circuit. In Fig. 6 *A* and *B*, right-hand panels, the theoretical time course of i_f was calculated in the case of zero series resistance (see Appendix A). The value of series resistance R_s calculated by solution of the circuit shown in Fig. 6*C* was 12·2 MΩ, a value which is as expected somewhat larger than the pipette resistance of about 3 MΩ. The increase in pipette resistance after sealing onto the membrane is a known phenomenon (Marty & Neher, 1983), and can be attributed to the partial plugging of the pipette that occurs when the cell membrane is sucked into its tip. As is shown in Fig. 6*D* by plotting the *I–V* relations for i_f in the three conditions illustrated in *A* and *B*, a full compensation of the series resistance would have resulted in a fairly large increase of i_f (about 2 times at −65 mV and 1·5 times at −115 mV).

Distortion of the voltage records was observed in the absence of series-resistance compensation in two other cells less completely analysed. These data show that the presence of an uncompensated series resistance can distort the time course and markedly decrease the measured size of i_f during voltage clamp analysis. Correction for the series resistance is obviously especially important when the amplitude is measured with the aim of calculating the current contribution to the cell's electrical activity.

DISCUSSION

The main findings of this work are that: (a) in the cells studied the net background current is outward at voltages in the range −61 to −35 mV and cannot therefore contribute to the diastolic depolarization in this range and (b) i_f is the only time-

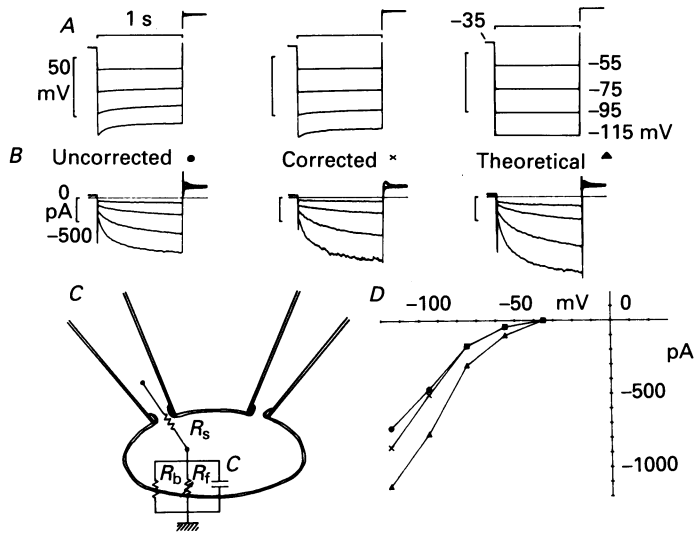

Fig. 6. Measurement of the i_f reduction due to uncompensated series resistance. Two pipettes were used in the whole-cell configuration on the same cell, as schematically depicted in panel *C*. While the pipette on the right-hand side only measured the membrane voltage (records in *A*), the one on the left-hand side was used to apply voltages and measure currents (records in *B*). *A* and *B*, voltage records (in *A*) measured by the 'voltage' pipette during hyperpolarizations to the range −55 to −115 mV from −35 mV displayed a time-dependent 'sag' which increased with step size in the protocol with no compensation (left). Partial compensation for the series resistance (middle) led to reduction of the voltage sag and increase of recorded i_f (*B*). Further increase of i_f was obtained in a theoretical calculation based on the circuit assumed in panel *C* (where R_s, R_b and R_f represent the series resistance and the membrane background and i_f resistances, respectively, see Appendix) on the assumption that $R_s = 0$ (right). *D*, *I–V* relations for i_f activated by 1 s pulses in the uncorrected (●), partially corrected (×) and theoretical protocols (▲).

dependent inward component activated and therefore the only inward contribution to the net current measurable in this range. Also, in agreement with previous results, it is found that the voltage range of activation of Ca^{2+}-dependent currents is too depolarized to affect the initiation of diastolic depolarization. Besides the lack of evidence for other inward components in the appropriate voltage range, the conclusion that i_f is the current responsible for generating the pacemaker depolarization is based on evidence that the size of i_f in the diastolic range exceeds that required to drive the depolarization (Figs 2 and 4).

Arguments against the i_f-activation hypothesis in previous work were based essentially upon two assumptions: (1) the too negative range of i_f activation, and (2) the existence of a background component with very low contribution from K^+ ions, responsible for setting the zero-current voltage near −35 to −40 mV (Brown, 1982;

Noma, Nakayama, Kurachi & Irisawa, 1984; Noble, 1984). In this paper it has been shown that these assumptions do not hold in the SA node myocytes studied. Activation of i_f can start at voltages as depolarized as -35 or -40 mV (DiFrancesco *et al.* 1986; DiFrancesco & Noble, 1989) and, as shown in Figs 2 and 4, the i_f activated during 100 ms steps is sufficiently large to underlie the pacemaker phase. Also, the i_f size is underestimated in the absence of a full correction for the series resistance (Fig. 6). Measurement of the background component, on the other hand, is seriously affected by the presence of a leakage conductance, which causes an inwardly directed shift of the instantaneous I–V relation (Fig. 5). Even in the best of cases, i.e. when the leakage is only attributable to the seal conductance, the apparent reversal potential of the instantaneous I–V relation can be shifted by as much as 5 mV with respect to its real value, as shown in Fig. 5. If then the true reversal potential for the background component is close to -66 mV, the possibility that the generation of the pacemaker depolarization relies on the presence of an inward background current unmasked by i_K can be excluded. It is important to note in this respect that if the net inward current required to drive the diastolic depolarization is small (of the order of a few picoamperes), the individual inward current responsible for this process must be substantially larger if it has to overtake the current i_K during its decay. In other words, the size of the current i_K needs to be added to the required net current value to obtain the individual inward component flowing during the pacemaker depolarization. Previous attempts at evaluating the contribution of i_f and other components to the pacemaker depolarization in single SA node cells had also indicated the primary relevance of i_f (van Ginneken, 1988; but see Nathan, 1987).

CONCLUSION

The data collected in this paper indicate that the current responsible for initiating the diastolic depolarization ('pacemaker' current) is the hyperpolarization-activated current i_f. Several lines of evidence suggest that the properties of i_f are appropriate for a component responsible for pacemaking. First, kinetics and ionic properties are appropriate for the generation of depolarizing processes in response to hyperpolarization (DiFrancesco, 1985). Further, the i_f activation threshold (about -35 to -40 mV) in the SA node coincides approximately with the zero-current voltage of these cells, suggesting that their depolarized zero-current potential is due to the presence of i_f rather than to an unspecified background component. Secondly, i_f is strongly modulated by both cholinergic and adrenergic neurotransmitters, in a way that ensures a fine regulation of rhythm through the slope of pacemaker depolarization (Brown, DiFrancesco & Noble, 1979; DiFrancesco & Tromba, 1988*a*,*b*; DiFrancesco, Ducouret & Robinson, 1989). If pacemaking were to be regulated according to the i_K-decay hypothesis, by a background conductance for which there is no evidence of modulation by neurotransmitters, an efficient control of pacemaking could obviously not be performed. Even more paradoxically, the effect of β-adrenergic stimulation would be to slow pacemaking as a result of the increase of i_K known to occur under the influence of catecholamines (Pappano & Carmeliet, 1979; Brown, McNaughton, Noble &Noble, 1975; Brown *et al.* 1979; Bennet, Mckinney, Begenisich & Kass, 1986; Giles, Nakajima, Ono & Shibata, 1989; Duchatelle-Gourdon, Hartzell & Lagrutta, 1989).

Protocols for evaluating the contribution of i_f to the pacemaker depolarization (see for example Doerr, Denger & Trautwein, 1989) depend on the availability of a specific i_f blocker. Although such a blocker is still unknown, and it is therefore not yet possible to evaluate the effect of a complete removal of i_f on the action potential configuration, low doses of ACh specifically inhibiting i_f (up to 30 nM and possibly higher) can possibly be used to discern the action of a partial suppression of i_f (see DiFrancesco *et al.* 1989).

APPENDIX A

In the solution of the circuit in Fig. 6*C*, the membrane capacity C can be ignored when considering slow i_f transients only. In this case the time dependence of the total recorded current, $i_t(t)$, is described as:

$$i_t(t) = i_b + i_f(t) = V_c/[R_s + R_f R_b/(R_f + R_b)] = V_m(t)[1/R_b + 1/R_f(t)], \quad \text{(A 1)}$$

and the membrane voltage $V_m(t)$ will be a function of the command voltage V_c according to the relation:

$$V_m(t) = V_c/(1 + R_s/R_b + R_s/R_f) \quad \text{[eqn (2) of text]}. \quad \text{(A 2)}$$

Here i_b and i_f are the currents through background time-independent (R_b) and time-dependent (R_f) elements, respectively. At $t = 0$ i_f is fully deactivated and $R_f = \infty$, so that from eqn (A 1):

$$R_s + R_b = V_c/i_{t0}, \quad \text{(A 3)}$$

and

$$1/R_b = i_{t0}/V_{m0}, \quad \text{(A 4)}$$

Where i_{t0} and V_{m0} are total current and membrane voltage at zero time, respectively. An equivalent relation is obtained from eqn (A 2):

$$V_{m0} = V_c[1/(1 + R_s/R_b)]. \quad \text{(A 5)}$$

At $t = \infty$ the membrane voltage V_m and R_f resistance will tend to asymptotic values V_m and R_f. Using relations (A 2) and (A 5):

$$V_c/V_m = R_s/R_f + V_c/V_{m0}. \quad \text{(A 6)}$$

On the simplifying assumption that i_f activation does not depend upon R_s, or, in other words, that the i_f kinetics are not altered by distortion of the voltage time course, the theoretical time course of i_f in the hypothesis of full R_s compensation is described as:

$$i_{ft}(t) = (V_c/V_i(t)) * i_f(t),$$

from which, using eqns (A 1) and (A 2), the total measurable theoretical current is derived as:

$$i_{tt}(t) = i_{ft}(t) + i_{t0} = V_c(i_t(t)/V_m(t) - i_{t0}/V_{m0}) + i_{t0}. \quad \text{(A 7)}$$

This equation was used in the calculation of the theoretical time course of current in Fig. 6. Values of R_b, R_s and R_f can be directly calculated from relations (A 3), (A 4) and (A 5).

APPENDIX B

BY D. NOBLE, J. C. DENYER AND D. DiFRANCESCO

Numerical reconstruction of spontaneous activity in the i_f-activation hypothesis

In this Appendix action potentials were reconstructed by numerical computation using the OXSOFT-HEART software package. The equations used were the same as in

Noble, DiFrancesco & Denyer, 1989, with modifications based on the experimental results summarized in Figs 2, 4 and 5. These were made to meet the following conditions: (1) at −35 mV, the net steady-state current should be outward; (2) the instantaneous current, as measured by voltage clamping from −35 mV, should have

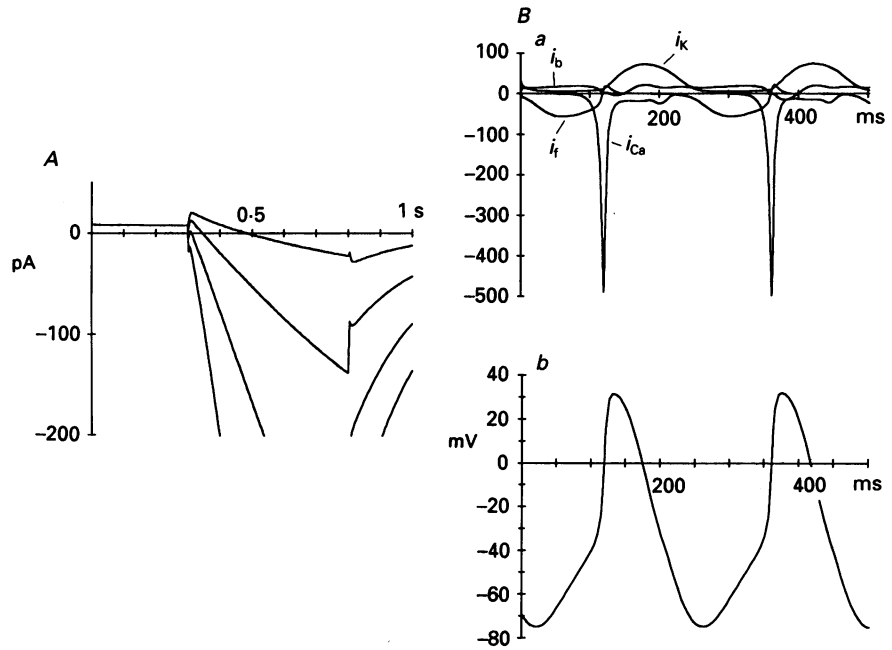

Fig. 7. *A*, computed current during voltage clamp steps from a holding potential of −35 mV to the range −45 to −75 mV in 10 mV steps. The model parameters were the same as in Noble *et al.* 1989, with the following modifications: mid-point voltages of activation–deactivation curves were −13 mV (Ca^{2+} current activation), −34 mV (Ca^{2+} current inactivation), −56 mV (i_f) and 0 mV (i_K); saturating value of i_K was 400 pA, for an external K^+ concentration of 5·4 mM; maximal pump current was 150 pA; conductances of background components were 0·08 pA/mV (Na^+) and 0·13 pA/mV (K^+). *B*, spontaneous action potentials (*b*) and corresponding ionic currents (*a*) computed with the above settings. The contributions of i_f, i_K, i_{Ca} and of the background component i_b (obtained as a sum of all remaining components except the fast Na^+ current) are labelled. Notice that i_f is the only inward current for the largest fraction of the diastolic depolarization.

a region of negative slope down to about −45 mV and reverse in the vicinity of −65 mV (Fig. 5); (3) the slope of the instantaneous *I–V* relation at voltages negative to −45 mV should be in the range of 0·05 pA per pF and mV (Fig. 5). Also, the positions of the mid-points of activation and deactivation curves for the Ca^{2+} current were set at −13 and −34 mV, respectively. A set of conditions satisfying the above requirements is listed in the legend of Fig. 7.

The computations were run for a SA node myocyte having a capacity of 27 pF (Noble *et al.* 1989). The aim of this computation is to show that the experimental data presented in this paper are compatible with the basic properties of the electrical activity of SA node cells. In particular, it is interesting to see how the generation and the elementary properties of spontaneous activity are interpreted in terms of the

'i_f-activation' hypothesis. In Fig. 7*A*, current records were computed during voltage clamp hyperpolarizations from a holding potential of −35 mV to the range −45 to −75 mV in 10 mV steps. These traces reproduce the main properties of the recorded data, and particularly the properties of the instantaneous component mentioned

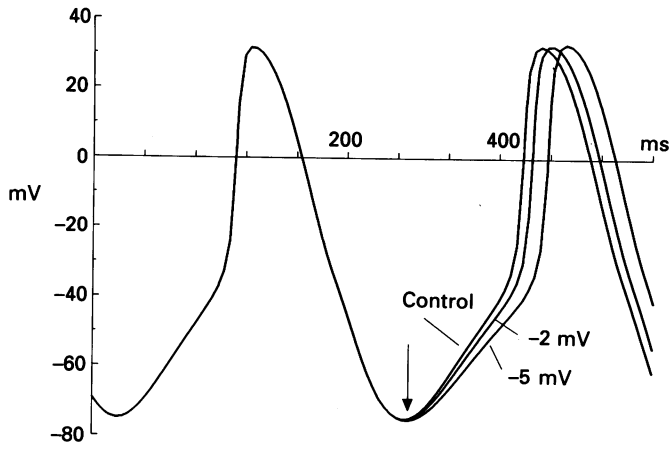

Fig. 8. Action potentials computed in standard conditions (control) and after shifting the i_f activation curve by −2 and −5 mV as indicated, at the time marked by an arrow, to simulate the action of ACh at 3 and 30 nM (see DiFrancesco *et al.* 1989, Fig. 2). The durations of the diastolic depolarization were approximately 12% and 39% longer, respectively, with the −2 and −5 mV shifts.

above. In Fig. 7*B* action potentials and ionic currents generated under the same assumptions are shown. Clearly, spontaneous activity can be generated even in the absence of an inward background current in the pacemaker range of voltages. In this case, as illustrated in the current plots, i_f supplies the inward current flow necessary for the initiation of the diastolic phase.

As an example of the ability of this model to fit experimental data, in Fig. 8 action potentials were calculated for a variety of conditions that correspond to different degrees of i_f inhibition, with the aim of representing the action of different concentrations of ACh.

The computations were performed after shifting the i_f activation curve by −2 and −5 mV which, according to the results of DiFrancesco *et al.* 1989, correspond approximately to the action of 3 and 30 nM-ACh. The slowing caused by these shifts is qualitatively similar to that obtained experimentally.

I should like to thank P. Lauricella, B. Pozzi, F. Porciatti and A. Malgaroli for assistance in some of the experiments, and I. S. Cohen for discussion and comments on the manuscript. This work was supported by the National Institute of Health (grant HL 35064) and the Consiglio Nazionale delle Ricerche (CT 88-00491-04-115-12810).

REFERENCES

ATTWELL, D., COHEN, I., EISNER, D., OHBA, M. & OJEDA, C. (1979). The steady-state TTX-sensitive ('window') sodium current in cardiac Purkinje fibres. *Pflügers Archiv* **379**, 137–142.

BEAN, B. P. (1985). Two kinds of calcium channels in canine atrial cells. *Journal of General Physiology* **86**, 1–30.

BENNET, P., MCKINNEY, L., BEGENISICH, T. & KASS, R. S. (1986). Adrenergic modulation of the delayed rectifier potassium channel in calf Purkinje fibres. *Biophysical Journal* **49**, 839–848.

BROWN, H. F. (1982). Electrophysiology of the sinoatrial node. *Physiological Reviews* **62**, 505–530.

BROWN, H. F., DIFRANCESCO, D. & NOBLE, S. J. (1979). How does adrenaline accelerate the heart? *Nature* **280**, 235–236.

BROWN, H. F., KIMURA, J., NOBLE, D., NOBLE S. J. & TAUPIGNON, A. (1984). The ionic currents underlying pacemaker activity in rabbit sino-atrial node: experimental results and computer simulations. *Proceedings of the Royal Society* B **222**, 305–328.

BROWN, H. F., MCNAUGHTON, P. A., NOBLE, D. & NOBLE, S. J. (1975). Adrenergic control of cardiac pacemaker currents. *Philosophical Transactions of the Royal Society* B **270**, 527–537.

DENYER, J. C. (1989). Isolation and electrophsiological characteristics of rabbit sino atrial node cells. D. Phil. Thesis, Oxford University Press, Oxford.

DIFRANCESCO, D. (1985). The cardiac hyperpolarizing-activated current, i_f. Origins and developments. *Progress in Biophysics and Molecular Biology* **46**, 163–183.

DIFRANCESCO, D. (1986). Characterization of single pacemaker channels in cardiac sino-atrial node cells. *Nature* **324**, 470–473.

DIFRANCESCO, D., DUCOURET, P. & ROBINSON, R. B. (1989). Muscarinic modulation of cardiac rate at low acetylcholine concentrations. *Science* **243**, 669–671.

DIFRANCESCO, D., FERRONI, A., MAZZANTI, M. & TROMBA, C. (1986). Properties of the hyperpolarizing-activated current (i_f) in cells isolated from the rabbit sino-atrial node. *Journal of Physiology* **377**, 61–88.

DIFRANCESCO, D. & NOBLE, D. (1985). A model of cardiac electrical activity incorporating ionic pumps and concentration changes. *Philosophical Transactions of the Royal Society* B **307**, 353–398.

DIFRANCESCO, D. & NOBLE, D. (1989). The current i_f and its contribution to cardiac pacemaking. In *Cellular and Neuronal Oscillators*, ed. JACKLET, J. W., pp. 31–57. M. Dekker, New York.

DIFRANCESCO, D., NOMA, A. & TRAUTWEIN, W. (1979). Kinetics and magnitude of the time-dependent potassium current in the rabbit sino-atrial node: effect of external potassium. *Pflügers Archiv* **381**, 271–279.

DIFRANCESCO, D. & TROMBA, C. (1988*a*). Inhibition of the hyperpolarization-activated current (i_f) induced by acetylcholine in rabbit sino-atrial node myocytes. *Journal of Physiology* **405**, 477–491.

DIFRANCESCO, D. & TROMBA, C. (1988*b*). Muscarinic control of the hyperpolarization-activated current (i_f) in rabbit sino-atrial node myocytes. *Journal of Physiology* **405**, 493–510.

DOERR, TH., DENGER, R. & TRAUTWEIN, W. (1989). Calcium currents in single SA nodal cells of the rabbit heart studied with action potential clamp. *Pflügers Archiv* **413**, 599–603.

DUCHATELLE-GOURDON, I., HARTZELL, H. C. & LAGRUTTA, A. A. (1989). Modulation of the delayed rectifier potassium current in frog cardiomyocytes by β-adrenergic agonists and magnesium. *Journal of Physiology* **415**, 251–274.

GILES, W., NAKAJIMA, T., ONO, K. & SHIBATA, E. F. (1989). Modulation of the delayed rectifier K^+ current by isoprenaline in bull-frog atrial myocytes. *Journal of Physiology* **415**, 233–249.

HAGIWARA, N., IRISAWA, H. & KAMEYAMA, M. (1988). Contribution of two types of calcium currents to the pacemaker potential of rabbit sino-atrial node cells. *Journal of Physiology* **395**, 233–253.

IRISAWA, H. (1978). Comparative physiology of the cardiac pacemaker mechanism. *Physiological Reviews* **58**, 461–498.

IRISAWA, H. (1987). Membrane currents in cardiac pacemaker tissue. *Experientia* **43**, 1131–1240.

MARTY, A. & NEHER, E. (1983). Tight-seal whole-cell recording. In *Single-Channel Recording*, ed. SAKMANN, B. & NEHER, E., pp. 107–122. Plenum Press, New York.

NATHAN, R. D. (1987). Role of i_f in pacemaker activity of the sino-atrial node. *Biophysical Journal* **51**, 263a.

NOBLE, D. (1984). The surprising heart: a review of recent progress in cardiac electrophysiology. *Journal of Physiology* **353**, 1–50.

NOBLE, D., DIFRANCESCO, D. & DENYER, J. (1989). Ionic mechanisms in normal and abnormal cardiac pacemaker activity. In *Neuronal and Cellular Oscillators*, ed. JACKLET, J. W., pp. 59–85. M. Dekker, New York.

NOMA, A., NAKAYAMA, T., KURACHI, Y. & IRISAWA, H. (1984). Resting K conductances in pacemaker and non-pacemaker heart cells of the rabbit. *Japanese Journal of Physiology* **34**, 245–254.

PAPPANO, A. J. & CARMELIET, E. E. (1979). Epinephrine and the pacemaker mechanism at plateau potentials in sheep cardiac Purkinje fibres. *Pflügers Archiv* **382**, 17–26.

VAN GINNEKEN, A. (1987). Membrane currents in mammalian cardiac pacemaker cells pp. 41–66. Doctoral Thesis, Rodopi, Amsterdam